Bremsstrahlung photons production for LUXE

Oleksandr Borysov
DESY (DE)
E-mail: oleksandr.borysov@desy.de

The LUXE experiment at DESY plans on using the European XFEL electron beam of 17.5 GeV in collision with a high intensity optical laser to study non-perturbative QED phenomena. One of the main phenomenon considered for experimental investigation is the rate of laser assisted electron-positron pair production in collisions of high energy photons with an intense laser beam. The present note reports on simulation studies of bremsstrahlung photon production as a possible source of high energy photons for LUXE.

1. Introduction

The proposed experiment LUXE (Laser und XFEL Experiment) aims to study non-perturbative QED processes in collisions of the European XFEL electron beam with an optical laser. Two such processes are considered for the design of the experiment setup: the laser assisted e^+ e^- pair production and the high intensity Compton scattering. A sketch of the experimental setup for the laser assisted pair production measurements is presented in figure 1. In this scenario, incident electrons of the XFEL beam hit a metal target to produce bremsstrahlung photons which then interact with a laser pulse. The spectrometer located after the target, followed by a colimator, is intended to register conversion electrons and positrons to estimate the number of produced bremsstralung photons.

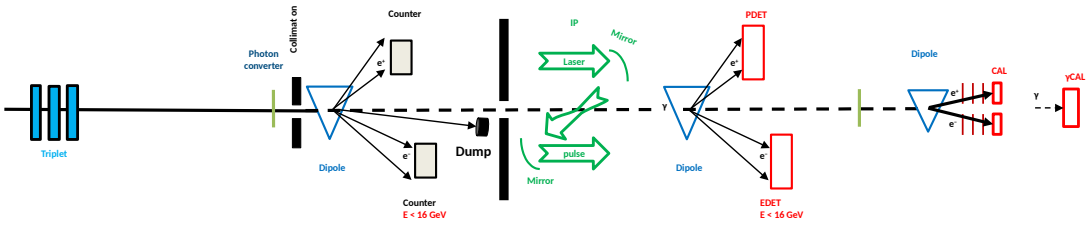

Figure 1: Diagram of the LUXE experiment layout designed for one photon pair production study.

This note describes the results of bremsstrahlung photons simulation obtained within the GEANT4 framework. Production rates, energy spectra and spacial distributions of bremssrahlung photons are investigated. The photon spectra are used as an input for modeling the interaction with a laser pulse at the LUXE interaction point (IP).

2. Simulation Model

The simulation is performed with GEANT4 [1] version 10.02.p02. The code is based on the TestEm5 example which was further extended to enable more settings for the primary particles. The geometry and output settings were also extended to meet the LUXE design and needs. The code can also be used for performance studies of the LUXE forward photon detector system which uses a dedicated target to convert photons into e^+e^- pairs. For this purpose the primary particles can be read from the list in an external file with arbitrary settings for particle type, momentum and position. In the LUXE case it would be the output from the simulation of electron – laser interaction which contains photons produced in high intensity Compton scattering.

For the bremsstrahlung production studies, the primary electrons are generated in accordance with the XFEL beam parameters [2]. Their values together with tentative numbers for the LUXE laser settings are presented in table 1.

From the solution of linearized equations, which describe the dynamics of beam particles in the plane transverse to the reference trajectory, the phase space for one of the transverse coordinates, x, is defined by the following equation [3]:

Table 1: LUXE laser and electron beam parameters at the IP.

Parameter	**Value**
Laser pulse energy (J)	3.5
Laser transverse size, $\sigma_x = \sigma_y$ (μm)	10.0
Laser pulse time (fs)	35
Electron beam energy (GeV)	17.5
Number of electrons ($\times 10^9$)	6.25
Electron beam transverse size, σ_x (μm)	5.0
Electron beam transverse size, σ_y (μm)	5.0
Electron beam duration (fs)	80
Electron beam normalized emittance (mm·mrad)	1.4
Crossing angle (rad)	0.3

$$\frac{1+\alpha^2}{\beta}x^2 + \beta x'^2 + 2\alpha x x' = A^2 \,, \tag{2.1}$$

where $x' = dx/dz$, A is an integration constant, β is an amplitude function which satisfies equation

$$2\beta\beta'' - \beta'^2 + 4\beta^2 K = 4 \,, \tag{2.2}$$

and α is defined by

$$\alpha = -\frac{1}{2}\beta' \,. \tag{2.3}$$

The coefficient K in equation (2.2) is determined by the particle charge, its momentum and the magnetic field. In the drift section, where the magnetic field is zero, $K = 0$, and the equation has the following solution:

$$\beta = \beta^* + \frac{z^2}{\beta^*} \,, \,, \tag{2.4}$$

where z is the distance from the IP and β^* is the value of the β function at the IP.

Equation (2.1) describes an ellipse in the x, x' phase space with area πA^2. For accelerator beam the interior of that ellipse is populated by beam particles and its area divided by π is called emittance, denoted by ε. It is conserved in a linear transport system. The Gaussian distribution of beam particles in the x, x' plane can be described by the following probability density function (PDF):

$$f(x,x',z) = \frac{1}{2\pi\varepsilon}\exp\left[-\frac{1}{2\varepsilon}\left(\frac{1+\alpha^2(z)}{\beta(z)}x^2 + \beta(z)x'^2 + 2\alpha(z)xx'\right)\right] . \tag{2.5}$$

For the accelerator section close to the IP, after the focusing magnet where the beam motion is essentially a drift in empty space, the solution (2.4) may be inserted into (2.3) and (2.5) with the resulting PDF given by

$$f(x,x',z) = \frac{1}{2\pi\varepsilon}\exp\left[-\frac{(x-zx')^2}{2\varepsilon\beta^*} - \frac{\beta^* x'^2}{2\varepsilon}\right] . \tag{2.6}$$

This is a Gaussian distribution with variances $\varepsilon\beta^*$ and ε/β^* for x and x', respectively, and a mean value of zx' for x. Using the normalized emittance of the European XFEL LINAC, $\varepsilon_n = 1.4$ mrad·mm [2] and the transverse size of the beam at the IP, $\sigma^* = 5$ μm, one can determine β^* from the expression

$$\beta^* = \frac{\sigma^{*2}}{\varepsilon}, \tag{2.7}$$

where the emittance $\varepsilon = \varepsilon_n/\gamma$ with a Lorentz factor $\gamma = E_{beam}/m_e \approx 3.5 \times 10^4$.

The positions and momentum vectors of the primary particles are generated according to the PDF (2.6) using (2.7) and either GEANT4 or CLHEP library functions for random numbers with Gaussian distributions. The distribution of primary particles in the x, x' phase space generated 5.2 m upstream of the LUXE IP ($z = -5.2$ m) is presented in figure 2. Figure 3 shows the corresponding distribution after using GEANT4 to transport the particles to the IP through the vacuum. One can see that the final distribution matches the designed value for the electron transverse beam-size at the IP of $\sigma^* = 5$ μm.

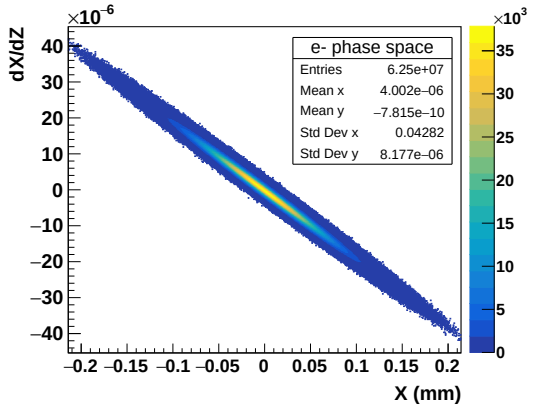

Figure 2: Phase space distribution of the primary electron beam 5.2 m upstream from interaction point.

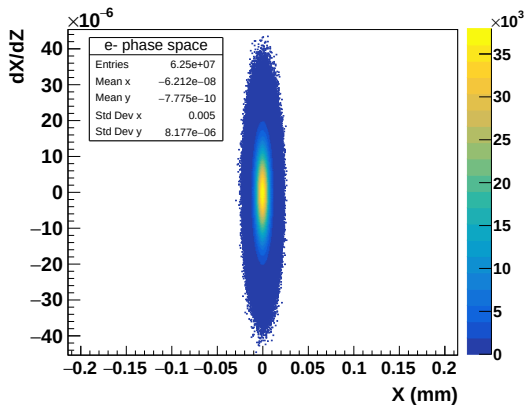

Figure 3: Phase space distribution of the electron beam at the interaction point.

The position in the other transverse coordinate, y, and the corresponding momentum component of primary electrons are generated in the same way. Correlations between x and y, if any, are not taken into account. The longitudinal position is also generated using a Gaussian distribution with $\sigma_z \approx 24$ μm independently of beam energy, which was fixed to 17.5 GeV.

It should be noted that the angular spread of primary electrons is defined by the normalized emittance of the European XFEL LINAC which is 1.4 mrad mm [2]. Considering the Lorentz factor $E_{beam}/m_e \approx 3.5 \times 10^4$ and the relationship between emittance and normalized emittance $\varepsilon = \varepsilon_n/\gamma$, the standard deviation of the Gaussian distribution for x' is $\sqrt{\frac{\varepsilon}{\beta^*}} = \frac{\varepsilon}{\sigma^*} \approx 8$ μrad. Similar numbers can be seen in figures 2 and 3 for the standard deviation of x'.

3. Simulation Results

The process of the laser assisted pair production in collisions of bremsstrahlung photons and laser beam was theoretically studied and results were presented in several papers [4, 5], just to

list a few. The spectrum of the bremsstrahlung photons was approximated using the following formula [3]:

$$\frac{dN_\gamma}{dE_\gamma} = \frac{X}{E_\gamma X_0}\left(\frac{4}{3} - \frac{4}{3}\frac{E_\gamma}{E_e} + \left(\frac{E_\gamma}{E_e}\right)^2\right), \tag{3.1}$$

where E_e is the energy of the incident electron, X_0 the radiation length of the target material and X is the target thickness. It is valid for thin targets as it neglects the photon to e^+e^- pair conversions within the target, and thus tends to overestimate the rate of high energy photons. It also does not contain information about the angular distribution of the bremsstrahlung photons. It is known that the beam is well collimated with a divergence inversely proportional to the Lorentz factor of the electron beam. Considering a rather small transverse size of the laser pulse and a relatively large distance between the target and the IP, the number of bremsstrahlung photons crossing the laser pulse might be significantly smaller than the total number estimated from (3.1). Figure 4 shows the spectra of bremsstrahlung photons produced in the GEANT4 simulation for a 35 μm ($1\%X_0$) thick tungsten target. The red line in the figure represents the spectrum of photons counted in the forward region with a position in the transverse plane limited to $\pm$1.5 m ($|x| < 1.5$ m and $|y| < 1.5$ m) at the IP, 2 m downstream of the target. It corresponds to projected polar angles of about 37°. The blue line corresponds to calculation using formula (3.1) which is in good agreement with the simulation. The green line shows the cross section for photons with a position in the transverse plane limited to ± 25 μm, which matches the transverse size of the LUXE laser beam with a reasonable overlap. The bottom ratio plot demonstrates that the number of photons which take part in the interaction with the laser beam constitutes only 5.15% of the total number of bremsstrahlung photons. The spacial distribution of photons in the IP plane is determined mainly by their angular spread in the production process and by multiple scattering of incident electrons in the target. Both of these effects are discussed later in more details. Since the initial electron beam is focused onto the IP and has a Gaussian shape with rather small $\sigma = 5$ μm in the IP transverse plane, the contribution of the initial electron angles is less significant.

The average number of bremsstrahlung photons produced per bunch crossing (BX) is about 5.6×10^8, the number of positrons – 1.6×10^6 and the total number of electrons observed behind the target is 6.26×10^9. The fact that for a thin target ($1\%X_0$) there is a good agreement between simulation and expectations of formula (3.1) is explained by the fact that the number of conversion positrons is by factor 100 less than the number of radiated photons. The spectra of positrons and electrons and their average numbers for one BX are presented in figure 5. These data are essential for background studies and for the development of a detector system to monitor the photon production by registering positrons.

The dependence of bremsstrahlung production on the material properties of the target, such as atomic number and mass density, is well approximated by a single parameter – the radiation length X_0. It follows, for example, from (3.1) and it is in good agreement with simulation (fig. 4). The spectra of bremsstrahlung photons produced in GEANT4 simulations with aluminum, copper and tungsten targets of $1\%X_0$ thickness were studied and found to be identical above 1 GeV. The area below 1 GeV looks slightly different for these targets with total number of photons in this region 23% higher for copper and 50% for aluminum compared to tungsten. At the same time it is shown in [4] that there is a lower bound on the energy of the photon for laser assisted pair

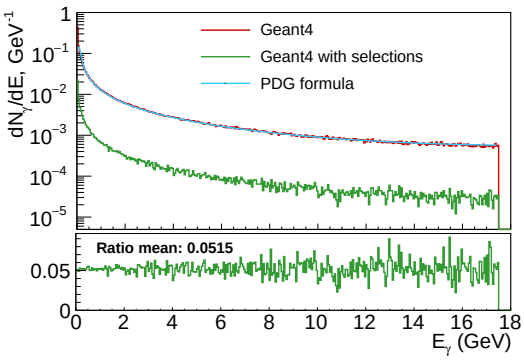

Figure 4: Comparison of bremsstrahlung spectra obtained from equation (3.1) and with GEANT4 simulation for a tungsten target of 35 μm (1%X_0) thickness. Green line shows the γ spectrum after imposing limits on position in the transverse plane to ± 25 μm which corresponds to the transverse size of the interaction area. The bottom plot shows the fraction limited by the interaction area.

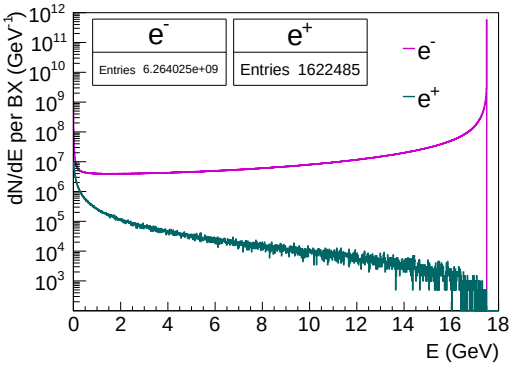

Figure 5: Spectra of electrons and positrons observed in the simulation with tungsten target of 35 μm (1%X_0) thickness for one bunch crossing.

production and for the LUXE conditions it is around 7 GeV. In this case the low energy photons are only relevant for the possible background study and have no influence on the pair production rate. For these reasons the tungsten is chosen as a target material for the simulation study. It has also other attractive properties: high melting point temperature, high thermal conductivity and high sputtering resistance.

Another parameter which is important for the experiment is the distance between the target and the IP. It is mainly constrained on the low side by the technical requirements for the electron and laser beam lines design in the vicinity of the LUXE IP and in the present study it is considered to be 5 m. It has also an effect on the thermal stability of the target because of the beam focusing. For 5 m distance, the Gaussian distribution of the beam electrons in the transverse plane has $\sigma \approx 43$ μm (figure 2) and it decreases as the distance between the target and the IP becomes smaller and consequently the heating power per unit volume increases.

The polar angle distributions of the bremsstrahlung photons for different energy domains are presented in figures 6, 7 and 8. The shapes of the distributions are similar for different energies. The distance of 5 m between the target and the IP, considering the transverse size ± 25 μm, corresponds to a projected polar angle of 5 μrad. The distribution in this area, shown in figure 8, can be well approximated by a uniform distribution. Consequently the number of photons interacting with the laser beam is proportional to the solid angle covering the IP in the transverse plane. This property allows using a simple formula for estimating the number of photons colliding with the laser beam for different distances between target and IP,

$$N_\gamma(R) = \frac{R_0^2}{R^2} N_\gamma(R_0)\,, \tag{3.2}$$

where R – the distance between the target and IP and $N_\gamma(R_0)$ is the number of photons for the distance R_0. Since the total number of photons in the forward region does not depend on the

distance, a similar formula is applicable for the estimation of the fraction of photons crossing the IP area. Calculating the fraction of photons for 5 m distance using the number 5.15% for $R_0 = 2$ m (figure 4) gives a fraction of 0.82% while the simulation gives 0.89%. A similar test for 12 m distance gives 0.15% considering $R_0 = 5$ m, 0.14% if $R_0 = 2$ m and the simulation result is 0.16%. It is clear that (3.2) is more accurate in the angular range where the curve in figure 8 is better approximated by a horizontal line.

The uniform spacial distribution of bremsstrahlung photons is also illustrated in figure 9 with projected distribution in the transverse plane at the IP within $|y| < 25$ μm.

It is worth noting that the observed flattening of the polar angle distribution in the proximity of zero cannot be explained by the bremsstrahlung production which in the GEANT4 simulation is considered to be independent of target material and energy of the incident particle and is approximated by the following PDF [6]:

$$f(u) = C\left(ue^{-au} + due^{-3au}\right), \tag{3.3}$$

where $u = \theta\gamma$ with γ – Lorentz factor of the incident particle and $C = 9a^2/(9+d)$, $a = 0.625$, $d = 27$ are numerical constants. As will be illustrated later in subsection 3.2, the angular distribution of bremsstrahlung photons is also affected by multiple scattering of the incident electrons in the target material.

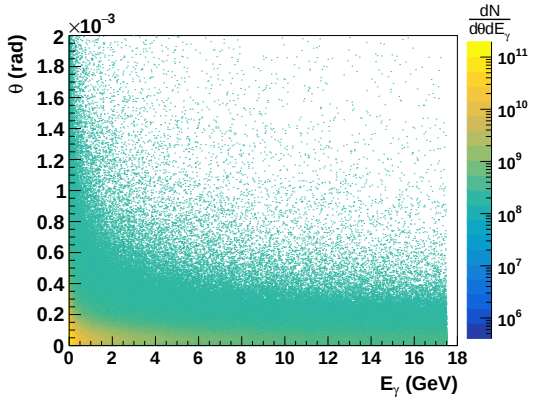

Figure 6: Distribution of bremsstrahlung photons in energy and polar angle plane for one BX, downscaled by a factor of 100.

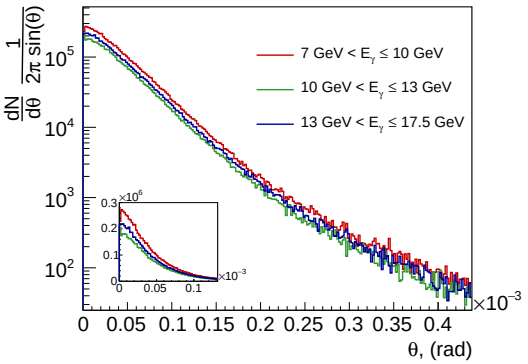

Figure 7: Polar angle distribution of bremsstrahlung photons in different energy ranges for one BX.

3.1 Target thickness

The thickness of the tungsten target of 35 μm ($1\%X_0$) was chosen mainly in order to compare the results of the MC simulation with those of the theoretical predictions [4] for laser assisted pair production rate. The theoretical approach uses formula (3.1), which provides accurate results only for thin targets, is found to be in a good agreement with GEANT4 simulation for a tungsten target of 35 μm (figure 4) and thus further simulation of photon interaction with a laser pulse would be comparable with the theoretical results. For the experiment, however, an increase of the photon flux can result in a higher rate of pair production and better statistics for studying physics processes

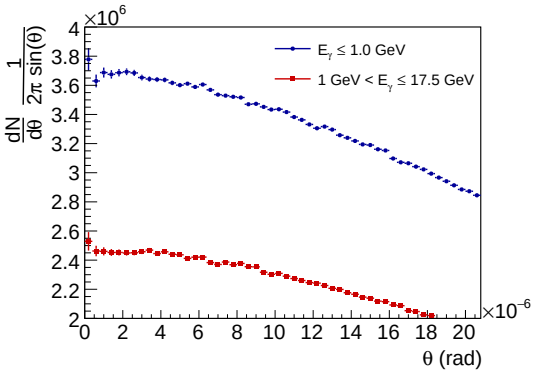

Figure 8: Polar angle distribution of bremsstrahlung photons for one BX within the area matching the IP transverse size.

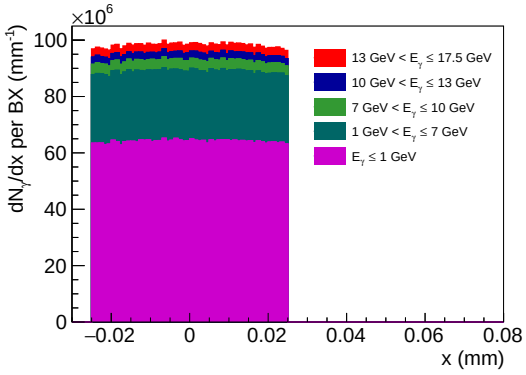

Figure 9: Bremsstrahlung photons position distribution in transverse coordinate x at the IP for $|y| < 25\mu$m.

in photon laser collisions. The number of bremsstrahlung photons can be altered by changing the thickness of the target.

Distributions of the number of photons obtained in simulation for tungsten targets of different thicknesses for 50 BX are presented in figure 10. Only photons with energy above 7 GeV in the area $|x| < 25\ \mu$m and $|y| < 25\ \mu$m around the IP are included. The average number of photons as a function of the target thickness is shown in figure 11. The simulation demonstrates that the number of high energy bremsstrahlung photons increases as the target becomes thicker up to about $25\%X_0$ where it nearly doubles compared to $1\%X_0$. For thicker targets, the rate of pair generation probably becomes significant and in combination with multiple scattering the number of high energy photons observed at the IP is reduced.

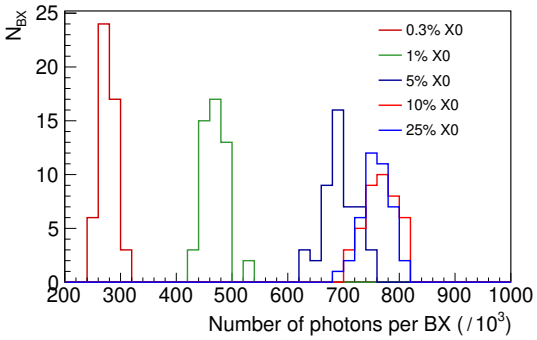

Figure 10: Number of bremsstrahlung photons in the energy range 7 GeV $< E_\gamma \leqslant$ 17.5 GeV expected at the LUXE IP from GEANT4 simulations of 50 bunches of the European XFEL electron beam of 17.5 GeV and tungsten targets of different thicknesses (for tungsten X_0 = 3.5 mm).

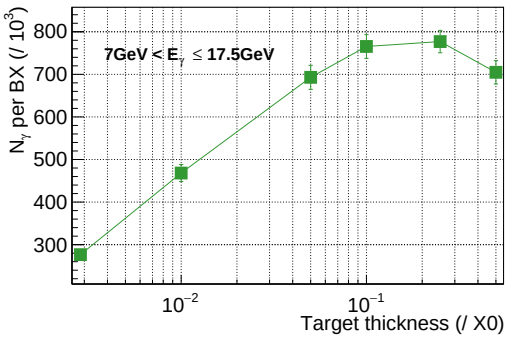

Figure 11: Average number of bremsstrahlung photons produced in the energy range 7 GeV $< E_\gamma \leqslant$ 17.5 GeV expected at the LUXE IP as a function of thickness of the tungsten target from GEANT4 simulation of 50 bunches of XFEL electron beam of 17.5 GeV.

3.2 Different physics models

GEANT4 provides classes which contain collections of implemented so-called reference physics lists. The present simulation study is based on the `G4EmStandardPhysics` class which is the default option for electromagnetic (EM) processes. It is included in the FTFP_BERT, QGSP_BERT and others physics lists which are widely used by the HEP experiments. There are several other classes for EM processes implemented in GEANT4 and the following two: `G4EmStandardPhysics_option3` and `G4EmStandardPhysics_option4` might be interesting to use for comparison. Both of these classes according to the documentation [7] provide EM physics for simulation with high accuracy. They use different models for multiple scattering compared to the `G4EmStandardPhysics` option, with specific algorithms for step limitation. `G4EmStandardPhysics_option4` contains an accurate angular generator for ionization models. Both of them use the same angular generator for bremsstrahlung `G4Generator2BS`.

For the comparison of simulated results of different physics lists, the 35 μm thick tungsten target is located 5 m upstream of the IP and an electron beam with a Gaussian distribution is used. 50 bunches are simulated with the number of electrons downscaled by a factor of 10^3. The distributions of the number of photons observed in the area $|x| < 25$ μm and $|y| < 25$ μm around the IP are presented in figure 12. It can be seen that in two different energy ranges, the average yield of bremsstrahlung photons is about 11% smaller for the `G4EmStandardPhysics_option3` physics list and about 21% smaller for the `G4EmStandardPhysics_option4` compared to the `G4EmStandardPhysics`. At the same time, when the geometrical selection criterium of 25 μm around the IP is dropped and all photons in the forward region within polar angle of about 17° are considered, the number of photons turns out to be identical for all the three physics lists, as shown in figure 13. Figure 14 shows the angular distribution of bremsstrahlung photons for different physics lists, where one clearly sees that it becomes wider for `G4EmStandardPhysics_option3` and `G4EmStandardPhysics_option4` compared to `G4EmStandardPhysics`.

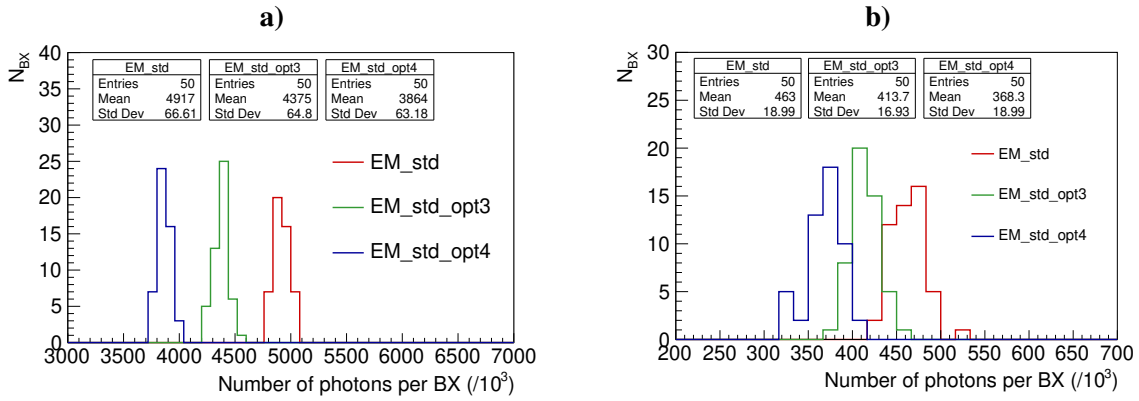

Figure 12: Number of bremsstrahlung photons observed in simulation with different GEANT4 physics lists at IP 5 m downstream from the target in the area limited to |x| < 25 μm and |y| < 25 μm. **a)** $E_\gamma < 17.5$ GeV; **b)** 7 GeV < E_γ < 17.5 GeV.

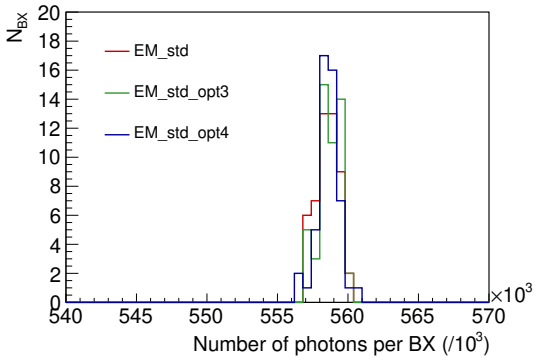

Figure 13: Distribution of the total number of bremsstrahlung photons observed in simulation with different GEANT4 physics lists in the forward area with polar angle less then 17°.

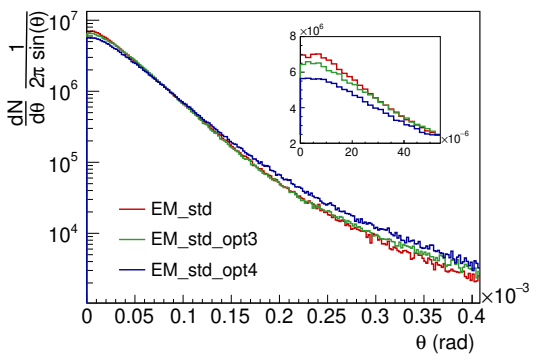

Figure 14: Polar angle distribution of bremsstrahlung photons observed in simulation with different GEANT4 physics lists.

4. Summary

A GEANT4 application has been developed to simulate bremsstrahlung radiation in collisions of an XFEL electron beam with a metal target to generate high energy photons used as input for a laser assisted pair production simulation study for the LUXE experiment.

The average number of particles for a tungsten target of 35 μm thickness and one bunch crossing of XFEL electron beam is presented in table 2. Electrons and positrons produced in the target can be deflected by a magnet and used for monitoring the number of high energy photons. In that case the numbers of electrons and positrons behind the target in the table provide an input for the design of a monitoring detector system and for background studies.

It has been demonstrated that the choice of a GEANT4 physics list for bremsstrahlung simulation can be a source of systematic uncertainty of up to 20% for the estimation of the number high energy photons at the LUXE IP.

The number of photons at the LUXE IP for different distances to the target can be estimated using (3.2) with an accuracy better than 5% for distances more than 5 m. Shorter distances would have an advantage for physics studies with LUXE, but it may not be possible due to technical constraints on the IP equipment. The number of photons can be slightly increased by using targets thicker than $1\%X_0$, but it saturates at $25\%X_0$, considering photons above 7 GeV inside the area defined by the size of the IP in the transverse plane.

Table 2: Average number of expected particles in the LUXE setup.

Particle	**Incident on the target**	**In forward region behind the target**	**At IP**
e^-	6.25×10^9	6.26×10^9	-
γ	-	5.60×10^8	4.91×10^6; (4.67×10^5, E>7GeV)
e^+	-	1.62×10^6	-

References

[1] J. Allison, et al. *Recent developments in GEANT4*, NIM A 835 (2016) 186.

[2] *List of Beam Parameters for the XFEL LINAC*, http://xfel.desy.de/technical_information/electron_beam_parameter

[3] M. Tanabashi et al., *(Particle Data Group)*, Phys. Rev. D 98 (2018) 030001.

[4] A. Hartin, A. Ringwald, and N. Tapia, *Measuring the boiling point of the vacuum of quantum electrodynamics*, Phys. Rev. D 99 (2019) 036008. arXiv:1807.10670.

[5] T.G. Blackburn and M. Marklund, *Nonlinear Breit-Wheeler pair creation with bremsstrahlung γ rays*, 2018 Plasma Phys. Control. Fusion 60 054009.

[6] *GEANT4 Physics Reference Manual* Section 8.2 Bremsstrahlung. http://GEANT4-userdoc.web.cern.ch/GEANT4-userdoc/UsersGuides/PhysicsReferenceManual/BackupVersions/V10.2/fo/PhysicsReferenceManual.pdf

[7] *GEANT4 User's Guide for Application Developers.* Section 5.2.1. Electromagnetic Interaction. http://GEANT4-userdoc.web.cern.ch/GEANT4-userdoc/UsersGuides/ForApplicationDeveloper/BackupVersions/V10.2/fo/BookForAppliDev.pdf